ACS APPLIED MATERIALS & INTERFACES

Research Article

www.acsami.org

Cationic Conjugated Polymer/Fluoresceinamine-Hyaluronan Complex for Sensitive Fluorescence Detection of CD44 and Tumor-Targeted Cell Imaging

Yanqin Huang,*[,†] Xin Yao,[†] Rui Zhang,[§] Lang Ouyang,[†] Rongcui Jiang,[†] Xingfen Liu,[†] Caixia Song,[†] Guangwei Zhang,[†] Quli Fan,[†] Lianhui Wang,[†] and Wei Huang*[,†,‡]

[†]Key Laboratory for Organic Electronics & Information Displays (KLOEID) and Institute of Advanced Materials (IAM), Nanjing University of Posts & Telecommunications, Nanjing 210023, China

[‡]Jiangsu-Singapore Joint Research Center for Organic/Bio- Electronics & Information Displays and Institute of Advanced Materials, Nanjing Tech University, Nanjing 211816, China

[§]Department of Ophthalmology, Zhongda Hospital, Southeast University, Nanjing 211189, China

Supporting Information

ABSTRACT: Simple, rapid, and sensitive detection of CD44 is of paramount importance since it plays pivotal roles in tumor initiation, growth and metastasis. Herein, we describe a novel method for sensitive, visual and facile fluorescence detection of CD44 and CD44-mediated cancer cell imaging, using a probe based on cationic conjugated polymer (CCP)—PFEP and fluoresceinamine-hyaluronan (FA-HA). HA is an anionic natural glycosaminoglycan that can specifically bind to the overexpressed CD44 on various kinds of cancer cells. PFEP and FA-HA formed a complex through electronic interactions, resulting in a highly efficient fluorescence resonance energy transfer (FRET) from PFEP to FA-HA; moreover, the efficiencies of FRET correlated with the concentrations of CD44 because the specific binding of HA-CD44 would separate FA-HA away from PFEP. This method did not require laborious and expensive dual-labeling or protein-labeling needed in previously reported detection methods of CD44. Just mix the sample and test solution containing the PFEP/FA-HA complex, and the results allowed naked-eye detection by observing fluorescent color of solutions with the assistance of a UV lamp. Most importantly, the use of a conjugated polymer with excellent amplification property as well as the specific binding of HA-CD44 endowed this method with high sensitivity and specificity, making it applicable for reliable quantitative detection of CD44. Furthermore, the PFEP/FA-HA complex formed nanoparticles in aqueous solution, and the nanoparticles can be selectively taken up by MCF-7 cells (cancer cell) through the HA-CD44 interaction, thereby giving rise to a dual-color tumor-targeted imaging probe with good photostability. The development of this fluorescent probe showed promising potential to make a reliable and routine method available for early diagnosis of cancer.

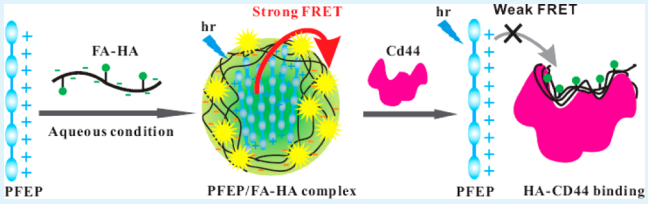

KEYWORDS: *cationic conjugated polymer, fluoresceinamine-hyaluronan, CD44, fluorescence resonance energy transfer (FRET), cell imaging*

INTRODUCTION

Hyaluronan (HA) is an anionic linear glycosaminoglycan composed of repeating disaccharide units of β-(1,4)-D-glucuronic acid and β-(1,3)-N-acetyl-D-glucosamine.[1,2] HA is abundant in extracellular matrices and synovial fluids and implicated in a wide variety of important biological processes, including tissue hydration, cell motility, proliferation, and differentiation.[2−4] Moreover, HA is a highly efficient molecule that can specifically bind to the receptor—CD44, which is overexpressed on various kinds of cancer cells.[2−4] This important characteristic of HA, along with its biocompatibility, biodegradability, and easily modified structure, makes HA-based materials extremely attractable for tumor-targeted delivery of imaging agents, cancer diagnosis, and therapy.[5−14]

CD44 is a major adhesion protein for the extracellular matrices. It has been involved in many physiological processes, such as lymphocyte homing and activation, wound healing, and cell migration.[1,15] Moreover, CD44 has sparked tremendous research interests as the target receptor for cancer diagnosis and therapy since it plays pivotal roles in tumor initiation, growth, and metastasis.[1,15−17] For example, the concentration of CD44 in the serum is elevated in patients with gastric or colon cancer, which was about 10 times that in the serum of normal individuals. Thus, CD44 concentration was reported to be an indicator of tumor burden and metastasis in patients with

Received: August 1, 2014
Accepted: October 3, 2014
Published: October 3, 2014

Scheme 1. (a) Schematic Illustration of the Overall Strategy for CD44 Detection and (b) Chemical Structures of FA-HA and PFEP

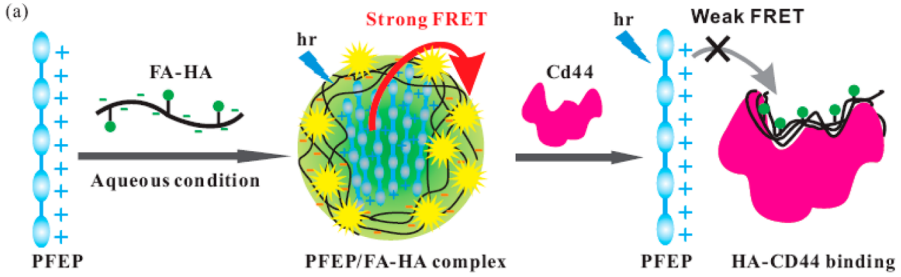

(b)

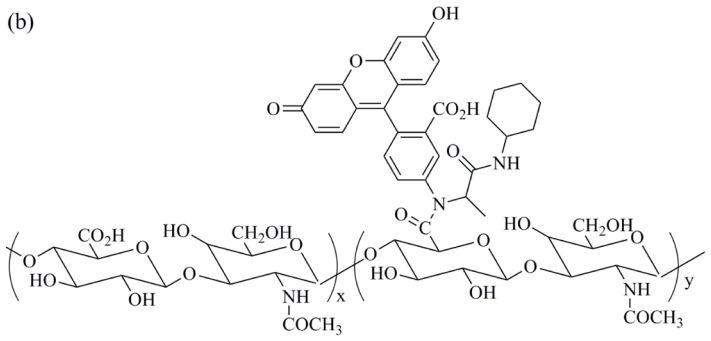

FA-HA

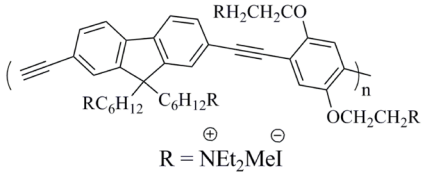

PFEP

malignant diseases.[18,19] Some noninvasive methods based on CD44 detection for tumor diagnosis have been reported, such as reverse transcription-PCR (RT-PCR),[20] Western blotting,[21] and ELISA assays.[18,22−26] Although these methods were superior to previous invasive methods in terms of comfortableness and simplicity, they are still inconvenient for routine diagnostic use.[26] They always required complicated procedures such as dual-labeling or protein-labeling, making these techniques time-consuming and expensive. Therefore, simple, rapid, and sensitive methods to detect CD44 are still highly desired. In addition, cancer stem cells, limited numbers of dedicated cells in a tumor, are capable of self-renewal and fuelling the growth of tumors, and CD44 has recently been identified as one significant cell surface marker associated with cancer stem cells in various types of tumors, such as breast, liver, head, neck, pancreas, and bladder cancer.[15,27] Hence, various HA-based derivatives have recently been investigated in cell imaging for cancer diagnosis via specific binding of HA to CD44.[5−14] The fluorescence technique is one of the most useful analytical tools in bioanalysis and imaging because it offers real-time and specific insight into cellular events with high sensitivity.[12,28] In previous studies, HA has often been labeled with organic fluorescent dyes[5−12] or quantum dots (QDs)[29,30] as optical imaging agents. Although these studies provided lots of valuable information, fluorescent dyes may not be suitable for long-time observation due to photobleaching,[31] and QDs suffer from celluar toxity by leaching harmful metals from the nanocrystal core.[32,33] There is still a great demand for novel HA-based optical imaging probes with better photostability and sensitivity.

Motivated by the above demands, we developed a novel, simple, and sensitve method for CD44 detection and tumor-targeted cell imaging, using a probe based on the fluorescent water-soluble conjugated polymer (WSCP)/fluoresceinamine-hyaluronan (FA-HA) complex. Over the past decade, WSCPs have established themselves as an efficient optical platform for sensing,[34−42] and very recently, various WSCPs have been proved useful for live-cell imaging.[43−54] WSCPs are synthetic macromolecules with fully conjugated backbones and hydrophilic polar side chains, which endow them with excellent photophysical and biophysical properties. On the one hand, in comparison to small molecule fluorescent dyes, the large, delocalized molecular structures result in higher luminescence brightness, better photostability, and optical signal amplification properties with efficient energy transfer mechanisms. On the other hand, amphiphilic WSCPs can form complexes with oppositely charged biomolecules through strong electrostatic and hydrophobic interactions, which is also very important for cellular interaction and subsequent cellular entry because the cell surface contains both negatively charged proteoglycans and hydrophobic membrane lipids. Moreover, it is also noted that WSCPs generally exhibit lower toxicity than most fluorescent dyes and QDs. Herein, a cationic conjugated polymer (CCP)—PFEP (Scheme 1)—with good photostability and excellent energy transfer properties was employed in our method, which can form a complex with anionic FA-HA, and efficient energy

dx.doi.org/10.1021/am505113p | ACS Appl. Mater. Interfaces 2014, 6, 19144−19153

transfer from PFEP to fluorescein subsequently occurred (Scheme 1). The FRET process triggered a "turn off" signal of blue and an amplified "turn on" signal of green. When CD44 was present, the specific binding of HA-CD44 separated FA-HA away from PFEP, and the fluorescence of PFEP recovered obviously. A multicolor optical sensor for CD44 was thus realized. Furthermore, the PFEP/FA-HA complex formed nanoparticles in aqueous solution, which was demonstrated by transmission electron microscopy (TEM). CD44-mediated tumor targeting behavior of the developed nanoparticles was evaluated in vitro through fluorescence cell imaging by using tumor cells and normal cells.

EXPERIMENTAL SECTION

Materials and Instruments. The water-soluble cationic conjugated polymer poly{[9,9-bis(6′-(N,N,N-diethylmethylammonium)-hexyl)-2,7-fluorenylene ethynylene]-*alt*-co-[2,5-bis(3′-(N,N,N-diethylmethylammonium)-1′-oxapropyl)-1,4-phenylene]} tetraiodide (PFEP) was synthesized according to a previously reported method.[55] The molecular weight and polydispersity of its neutral polymer are 12 600 and 1.28, respectively.

Sodium hyaluronate (M_w > 10^3 kDa) and sodium hyaluronate oligomer (M_w = 3−10 kDa) were purchased from Qisheng Biological Preparation Co., Ltd. (Shanghai, China) and Bloomage Freda Biopharm Co., Ltd. (Jinan, China), respectively. Cyclohexyl isocyanide and acetaldehyde were obtained from J&K Scientific Ltd. (Shanghai, China). Fluoresceinamine was purchased from Acros. CD44 was purchased from Immune Technology Corp. (Suzhou, China). Bovine serum albumin (BSA), thrombin, and lysozyme were ordered from Sigma. The serum was obtained from Zhongda Hospital and was frozen and stored at −75 °C until use. All other reagents were obtained from Sinopharm Chemical Reagent Co., Ltd. (Shanghai, China). All solutions were prepared using Milli-Q water (18.2 MΩ cm) from a Millipore system.

^{1}H NMR spectra were recorded on a Bruker Ultra Shield Plus 400 MHz NMR. UV−vis absorption spectra were recorded on a SHIMADZU UV-3600 spectrophotometer. Photoluminescence (PL) and FRET measurements were carried out using a SHIMADZU RF-5301PC spectrofluorophotometer with a xenon lamp as a light source. The hydrodynamic sizes of nanoparticles were determined by dynamic light scattering (DLS) using a 90 Plus particle size analyzer (Brookhaven Instruments). Zeta potentials were measured using a zeta potential analyzer (ZetaPALS, Brookhaven Instruments Corp). Transmission electron microscopy (TEM) images were recorded on a JEOL 2010 transmission electron microscope at an accelerating voltage of 100 kV. Fluorescence images were obtained with a confocal laser scanning microscope (CLSM, Leica, TCS SP5, Germany).

Methods. *Preparation and Characterization of Fluoresceinamine-Labeled Hyaluronate (FA-HA).* Fluoresceinamine-labeled hyaluronate was synthesized as described in the literature.[48] In brief, FA-HA was produced from a one-step condensation-rearrangement reaction involving FA, acetaldehyde, cyclohexyl isocyanide, and HA in a mixture of DMSO and H_2O at 22 °C. The product was characterized by gel filtration chromatography on a Sepharose CL-2B column equilibrated with PBS, and the purity was estimated to be 97%. The degree of substitution (DS, defined as the molar ratio of FA in FA-HA) was determined using two methods, including ^{1}H NMR[8,9,11] and a FA absorption standard curve.[56] The absorption standard curve was constructed for methyl N-fluoresceinylthiocarbamate in borate solution (pH 9) by plotting concentration against absorption at 492 nm. The FA-HA samples were dissolved in borate solution, and the absorption was measured. For ^{1}H NMR, the sample was prepared by dissolving the compound in D_2O. FA-HA samples were stored as the lyophilized solid in the absence of light at −20 °C.

CD44 Detection. For the detection of CD44, fluorescence spectrometric titration experiments were carried out at room temperature (25 °C) in a 700 μL quartz cuvette with an optical path length of 1.0 cm. CD44 dissolved in Milli-Q water was added successively to the buffer solution (10 mM tris-HCl,100 mM NaCl, pH 8.0) of PFEP/FA-HA complex ([PFEP] = 5.0×10^{-7} M, [FA-HA] = 4.0×10^{-6} M, the concentrations both refer to the molar concentrations of the polymer repeat unit). The FRET behaviors from PFEP to FA-HA were studied by comparison of FRET efficiencies of the solutions with CD44 at different concentrations. The FRET efficiency was evaluated by the ratio of acceptor (FA-HA) emission intensity to donor (PFEP) emission intensity.[57,58]

Preparation and Characterization of PFEP/FA-HA Complex Used in Cell imaging. PFEP and FA-HA were both dissolved in phosphate buffered saline (PBS, 0.02 M, pH 7.4) at room temperature ([PFEP] = 5.0×10^{-6} M, [FA-HA] = 5×10^{-4} M, HA oligomer was used in these experiments), and the solution was vortexed for 10 min and then sonicated for 20 min. Nanoparticle sizes were determined by TEM, and zeta potentials were also used to estimate the interaction between PFEP and FA-HA. A drop of sample solution was placed onto a 300-mesh copper grid coated with carbon and air-dried, and then the TEM images were taken. Furthermore, CD44 was added to the complex ([CD44] = 1×10^{-6} g/mL), and TEM images and zeta potentials were also measured to study the changes of nanoparticle sizes after the binding of CD44 with FA-HA. In all of these above experiments, a sample of PFEP solution with the same concentration was used as a control.

Cellular Uptake of PFEP/FA-HA Complex and Imaging. To evaluate cancer cell specificity of the PFEP/FA-HA complex, we tracked its cellular internalization in MCF-7 cells (cancer cell) and NIH-3T3 cells (normal cell). The cells were first cultured in confocal microscope dishes at a density of 5×10^5/mL in culture medium for 24 h at 37 °C. Then, the medium was replaced with the medium without FBS and containing the above PFEP/FA-HA complex. The final concentration of PFEP and FA-HA were 5.0×10^{-6} M and 5×10^{-4}, respectively. After incubation for 2 h at 37 °C, the cells were rinsed twice with PBS (0.01 M, pH 7.4). As a control experiment, another dish of MCF-7 cells was incubated with a high dose of free-HA ([HA] = 0.5 mg/mL) for 2 h at 37 °C before treatment with PFEP/FA-HA complex. The fluorescent images were all recorded on a confocal laser scanning microscope with excitation at 405 nm, and the emission in the ranges of 430−460 nm and 510−550 nm were recorded, respectively.

RESULTS AND DISCUSSION

Preparation and Characterization. In this paper, FA was conjugated to HA through a simple reaction to produce a dye-labeled polymer. The peaks for the N-acetyl group of HA (1.8 ppm) and the aromatic ring of FA (6.4−6.8 ppm) were confirmed in ^{1}H NMR spectra, indicating that FA-HA was successfully synthesized (Figure 1). The degree of substitution (DS), the introduction ratio of FA to HA, was estimated from the integration ratio of the peak of the aromatic ring of FA to that of the N-acetyl group of HA and was 5‰.[8,9,11] The level of HA labeling was also estimated using a FA absorption standard curve constructed for methyl N-fluoresceinylthiocarbamate by plotting concentration against absorption (492 nm). The molar ratio of FA in FA-HA was estimated to be 5.9‰, which was close to the value estimated using ^{1}H NMR spectra.

PFEP was composed of a fluorenyleneethynylene phenylene backbone with quaternary ammonium groups on the side chains, including both the 9,9 position of the fluorenylene unit and the 2,5 position of the phenylene unit. The photophysical property of PFEP was investigated in water. As shown in Figure 2, the absorption spectrum of PFEP exhibits a maximum peak at 405 nm. Upon excitation at 405 nm, the emission spectrum shows a maximum peak at 445 nm. Good overlap can be observed between the emission of PFEP and the absorption of FA-HA, which enables an efficient FRET from PFEP to FA-HA.[58,59] PFEP exhibits blue light emission in water with a high quantum yield of 26%. Moreover, PFEP was excited under

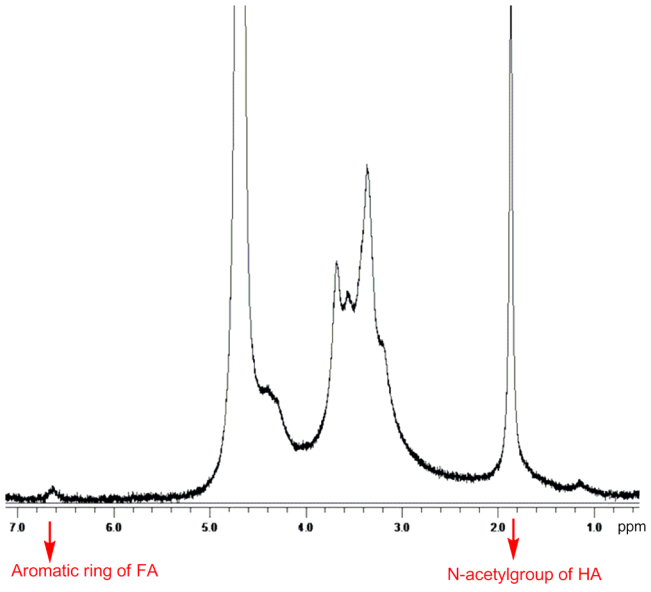

Figure 1. ^{1}H NMR spectrum of FA-HA.

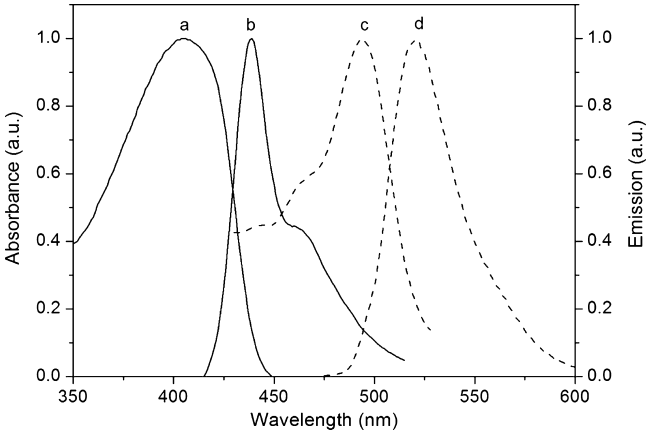

Figure 2. UV−vis absorption (a, c) and emission spectra (b, d) of PFEP (a, b) and FA-HA (c, d) in tris buffer solution (10 mM, pH 8.0).

continuous strong UV irradiation by a mercury lamp (100 W), and the fluorescence remained 60% after 25 s, which demonstrated that the photostability of PFEP was much better than many organic fluorescent dyes.[60] Therefore, PFEP was anticipated to be a good fluorescent signal reporter.

CD44 Detection. The strategy for CD44 detection was illustrated in Scheme 1. Cationic PFEP can form a complex with oppositely charged FA-HA through electrostatic interactions. Thus, the close proximity allowed for efficient FRET from PFEP to fluorescein conjugated with HA.[58,59] As a result, the fluorescence of FA-HA was significantly amplified with excitation at the maximum absorption of PFEP (405 nm), and the solution emitted green fluorescence. Upon adding CD44, the specific HA-CD44 binding separated FA-HA away from the complex.[2−4] In this case, FRET from PFEP to FA-HA was inefficient, and the blue emission of PFEP recovered. By monitoring the change of FRET ratio with the addition of CD44, it was possible to detect CD44 quantitatively. Meanwhile, changes in emission color can be observed by the naked eye under a portable UV lamp.

First, we did the following experiments to verify the feasibility of this strategy. As shown in Figure 3a, PFEP itself

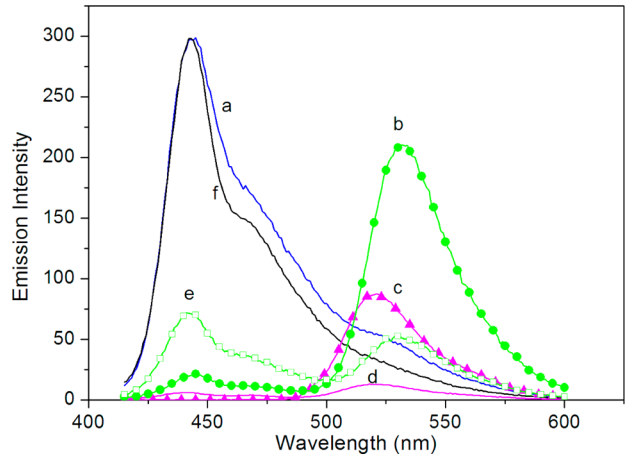

Figure 3. (a) Emission spectra of PFEP excited at 405 nm, (b) PFEP/FA-HA excited at 405 nm, (c) FA-HA excited at 492 nm, (d) FA-HA excited at 405 nm, (e) PFEP/FA-HA/CD44 excited at 405 nm, (f) PFEP/CD44 excited at 405 nm. Measurements were performed in tris buffer solution (10 mM, pH 8.0). [PFEP] = 5.0×10^{-7} M, [FA-HA] = 2.5×10^{-5} M, [CD44] = 7.5×10^{-6} g/mL.

([PFEP] = 5.0×10^{-7} M) in 10 mM tris-HCl (pH = 8.0) emitted strongly with a maximum at 445 nm when excited at 405 nm. The addition of FA-HA ([FA-HA] = 2.5×10^{-5} M) to the solution of PFEP led to a sharp decline of blue emission at 445 nm, and a prominent green emission appeared at 531 nm (Figure 3b). Specifically, the green emission intensity was about three times the intensity of FA-HA (Figure 3c) when excited without PFEP at its own absorption peak, 492 nm, and FA-HA itself emitted very weakly with excitation at 405 nm (Figure 3d). Moreover, Figure 3b also displayed clearly that the maximum of green emission (531 nm) was red-shifted 10 nm relative to its emission maximum (521 nm) when excited directly without PFEP (Figure 3c), consistent with the complex formation and an increase in polarity in the vicinity of fluorescein by the close proximity to PFEP.[46,55] All of these indicated clearly that energy transferred efficiently from PFEP to FA-HA with the formation of the complex and that the emission of FA-HA was significantly amplified. As shown in Figure 3e, after the addition of CD44 ([CD44] = 7.5×10^{-6} g/mL), the specific HA-CD44 binding was stronger than the electrostatic interactions in the PFEP/FA-HA complex; consequently, FA-HA was separated from the complex, the distance between PFEP and FA-HA increased, and FRET became inefficient. As a result, the green emission decreased obviously with the rise of the blue emission. In addition, CD44 was also added into the PFEP solution in the absence of FA-HA, and no obvious change was observed for the emission of PFEP (Figure 3f), which offered another confirmation of the HA-CD44 binding and FRET from PFEP to FA-HA.

Figure 4a showed the fluorescence spectra changes of PFEP/FA-HA ([PFEP] = 5.0×10^{-7} M, [FA-HA] = 4×10^{-6} M) with the successive addition of CD44 (normalized to the emission of PFEP, see Figure S1 for un-normalized data). In these experiments, the emission spectra were measured at 3 min intervals over 21 min with excitation at 405 nm, and the concentration of CD44 ranged from 1.0×10^{-8} M to 1.0×10^{-5} M. The initial solution of PFEP/FA-HA displayed a strong emission of FA-HA. Upon adding CD44, the emission of FA-HA at 531 nm gradually decreased with the increase of CD44 concentration and was almost quenched at the concentration of

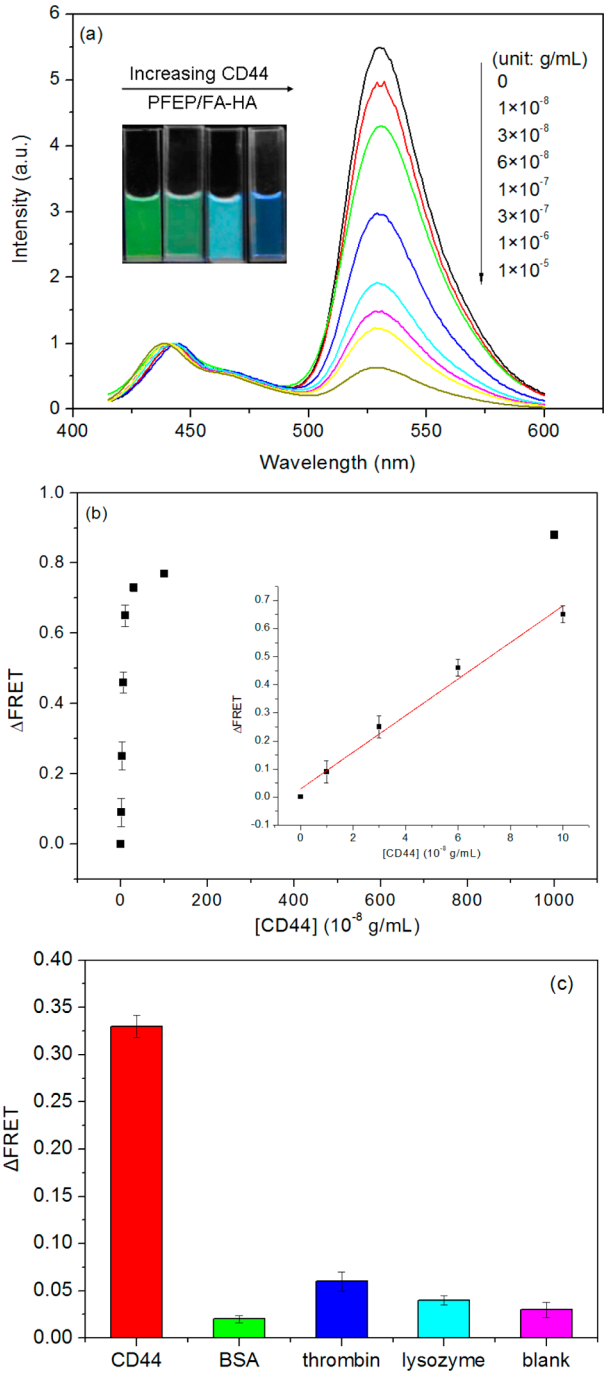

Figure 4. (a) Emission spectra of PFEP/FA-HA with the addition of CD44 (normalized to the emission of PFEP). The inset shows the photographs of PFEP/FA-HA solutions with increasing concentration of CD44 under a portable UV lamp with excitation at 365 nm. ([CD44] = 0, 3×10^{-7}, 1×10^{-6}, 1×10^{-5} g/mL). (b) Dependence of ΔFRET as a function of CD44 concentration. The inset shows the linear plot obtained in the concentration range from 0 to 1×10^{-7} g/mL. (c) Comparison of the ΔFRET for the detection of CD44 (4.5×10^{-8} g/mL), other proteins (BSA, thrombin, and lysozyme, each at 2×10^{-7} g/mL). Measurements were performed in tris buffer solution (10 mM, pH 8.0). [PFEP] = 5.0×10^{-7} M, [FA-HA] = 4×10^{-6} M.

1.0×10^{-5} M. Changes in the fluorescence spectra of PFEP/FA-HA could be monitored by the naked eye under a portable UV lamp with excitation at 365 nm. The inset of Figure 4a exhibited that the emission color of PFEP/FA-HA gradually changed from green to blue with increasing concentration of CD44 ([CD44] = 0, 3×10^{-7}, 1×10^{-6}, 1×10^{-5} g/mL). Thus, naked eye detection of CD44 was feasible with PFEP/FA-HA as a fluorescent probe. We also examined the changes of FRET ratio (I_{531nm}/I_{445nm}) using ΔFRET calculated from the following equation, where $FRET_0$ and FRET were the FRET ratio of PFEP/FA-HA complex in the absence and presence of CD44, respectively.

$$\Delta FRET = 1 - FRET/FRET_0$$

The dependence of ΔFRET as a function of CD44 concentration is shown in Figure 4b. ΔFRET increased sharply with the addition of CD44 and reached a plateau as the concentration became larger than 1×10^{-7} g/mL. The inset of Figure 4b showed that a linear plot was obtained in the concentration range from 0 to 1×10^{-7} g/mL. Thus, the limit of detection (LOD) was estimated to be 2.3×10^{-8} g/mL at a signal-to-noise ratio of 3. Moreover, we investigated the sensitivity of this strategy at different molar ratios of PFEP and FA-HA. As shown in Figure S2 and Table S1, when the concentration of FA-HA was 2.5×10^{-5} M, the largest $FRET_0$ was obtained in the absence of CD44. When the concentration of FA-HA decreased to 2.5×10^{-6} and 4.0×10^{-7}, the $FRET_0$'s were too low to be used for detection. By using the same method as above, linear plots were also obtained at the concentrations of 2.5×10^{-5} M and 4×10^{-5} M, and the linear range became wider with the increase of $FRET_0$. For example, at the concentration of 2.5×10^{-5} M, the linear range was from 0 to 1×10^{-6} g/mL and the LOD was estimated to be 1.7×10^{-7} g/mL (Figure S3).

Furthermore, in order to explore more fully the specificity of this strategy for CD44 detection, a series of control experiments were designed using bovine serum albumin (BSA), thrombin, and lysozyme. The results shown in Figure 4c exhibited that the addition of BSA, thrombin, and lysozyme did not produce the high ΔFRET observed for CD44 even though the concentration of the former (2×10^{-7} g/mL) was more than four times that of the latter (4.5×10^{-8} g/mL). This finding further confirmed that the proteins that did not bind to HA would not separate FA-HA from the complex, hence an efficient FRET signal would be maintained and ΔFRET was very low. Additionally, a blank experiment was also done using Milli-Q water. Milli-Q water with the same volume as that of CD44 was added to the solution of PFEP/FA-HA, and a very low ΔFRET was obtained, implying that the dilution of solution did not have much effect on the results of detection. Taken together, these results provided convincing evidence for the specificity of our fluorescent probe. The applicability of this strategy for the quantitative detection of CD44 in the serum was further evaluated. The serum was obtained from Zhongda Hospital. CD44 at different concentrations was then added to the serum, and a series of similar detection experiments were performed. Figure S4 showed very similar FRET efficiency responses for CD44 detection in the serum. The linear range was from 0 to 1 $\times 10^{-7}$ g/mL, and the LOD was estimated to be 3.5×10^{-8} g/mL. These results indicated that the other components in the serum have no obvious effect on the CD44 detection.

In Vitro Cellular Uptake of PFEP/FA-HA Complex. The results obtained from in vitro CD44 detection motivated us to further investigate the cellular uptake of the PFEP/FA-HA complex into cancer cell lines overexpressing CD44 by fluorescence microscopy. Before that, the microstructural characterization of the PFEP/FA-HA complex in PBS was

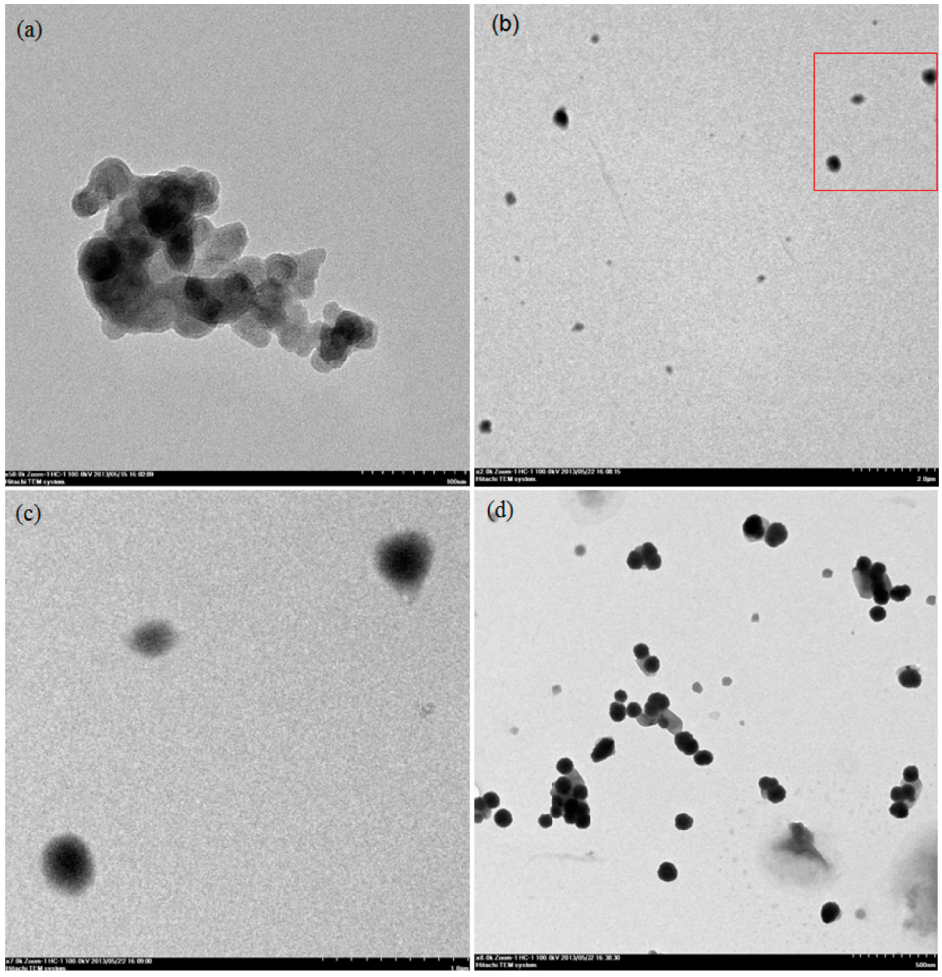

Figure 5. TEM images of (a) PFEP (scale bar: 100 nm), (b) lower magnification (scale bar: 2 μm), and (c) higher magnification (scale bar: 1 μm) of PFEP/FA-HA complex, (d) PFEP/FA-HA/CD44 system (scale bar: 500 nm).

performed. The sizes and surface charges of PFEP molecules in aqueous solution will be changed after binding with FA-HA, because the cationic side chains of PFEP provided electrostatic binding force to FA-HA. The sizes were therefore investigated by TEM. TEM in Figure 5a showed that amphiphilic PFEP itself formed nanoparticles with a size of about 50 nm, although the nanoparticles adhered to each other instead of dispersing well. After adding FA-HA, Figure 5b displayed that the diameters of the particle size obviously enhanced to the range of 200−350 nm, and Figure 5c with higher-magnification showed clearly that the nanoparticles were approximately spherical in shape with dark inner cores. Moreover, zeta potential of PFEP was around +35.96 mV in aqueous solution. After mixing with FA-HA in a molar ratio of 1:100, the zeta potential of PFEP/FA-HA complex changed to −87.53 mV. Hence, it was rational to speculate that the ionized carboxylic groups of HA most likely located in the shell.[9,11] All of these indicated that the PFEP/FA-HA nanoparticles, composed of a more compact hydrophobic inner core and hydrophilic shell, were successfully formed.[6,13,14] Furthermore, CD44 was added to the complex to investigate the changes of nanoparticles after the binding of CD44 with FA-HA. As shown Figure 5d, the mean diameters of nanoparticles reduced to around 100 nm, and the zeta potential also changed to −14.2 mV, providing direct proof that some of the FA-HA molecules were separated from the complex due to the strong HA-CD44 binding. These results were consistent with the phenomena observed in the above fluorescence spectrometric titration experiments.

There are some references reported in the literature which also work on the replacement technology for fluorescent DNA sensing by utilizing the structure switching among various forms of DNA,[61−65] such as a molecular beacon, a DNA double helix, and aptamer binding. However, most of them were limited to in vitro detection in homogeneous solution. By contrast, our method provided the possibility of diagnosis of cancer through cell imaging experiments due to the specific binding of HA and CD44. To verify this point, we evaluated the cellular uptake efficiency with the PFEP/FA-HA complex by CLSM studies in NIH-3T3 cells (mouse embryonic fibroblast cell) and MCF-7 cells (human breast cancer cell). It has been previously reported that NIH3T3 is the normal cell line with a low CD44 expression[10,14] and that MCF-7 is a cancer cell line with a high CD44 expression.[9,11,13] Thus, these cell lines were used without additional experiments to confirm the levels of CD44 expression. As shown in Figure 6a, strong fluorescent signals were detected in the cytoplasm for MCF-7 cells with excitation at 405 nm, indicating that PFEP/FA-HA nanoparticles were readily taken up by MCF-7 cells. In view of the specific HA-CD44 binding, the bright blue color should be attributed to the recovery of emission from PFEP, and the slightly dark green color was attributed to the emission of fluorescein due to the weak FRET from PFEP. In comparison,

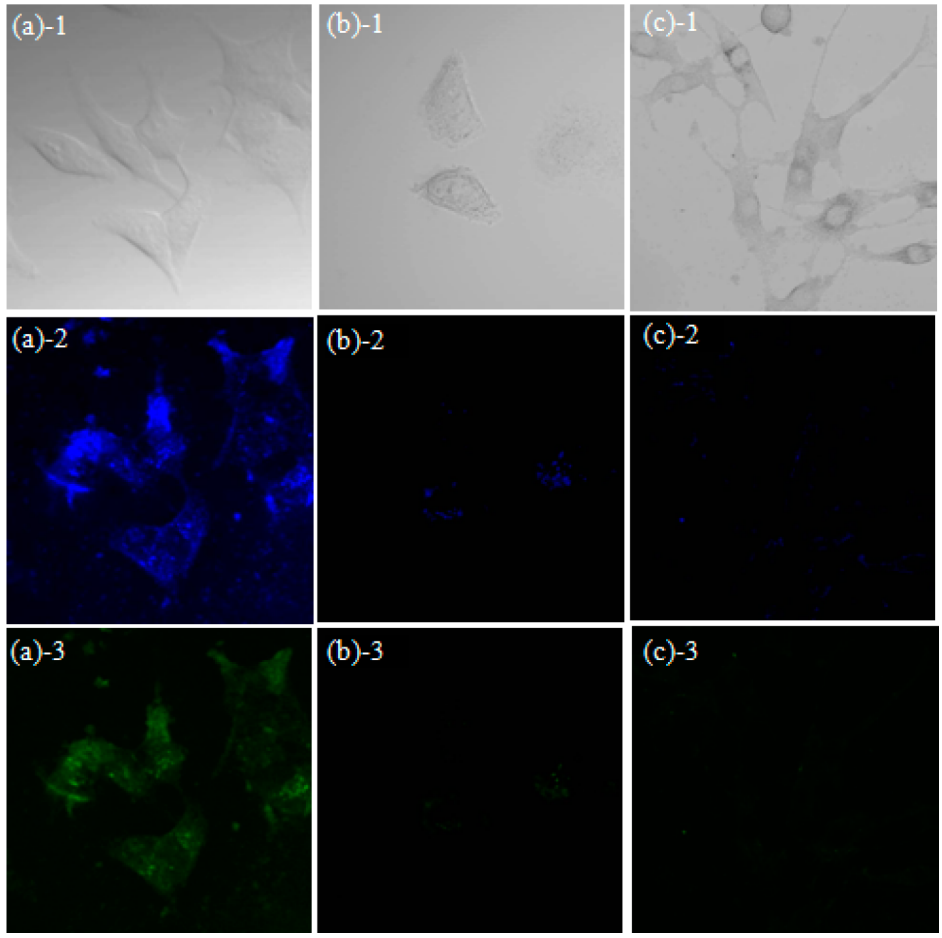

Figure 6. Phase contrast images (1) and fluorescent microscopic (2−3) images of MCF-7 cells (a), MCF-7 cells pretreated with HA (b), and NIH-3T3 cells (c) after incubatation with the PFEP/FA-HA complex for 2 h at 37 °C. Blue and green colors indicate the fluorescence of PFEP and fluorescein on FA-HA, respectively.

when the MCF-7 cells were pretreated with a high dose of free-HA to block CD44 before PFEP/FA-HA complex treatment, intracellular fluorescence was rarely observed in Figure 6b, suggesting a lack of cellular uptake of PFEP/FA-HA nanoparticles. Also, when the PFEP/FA-HA complex was incubated with NIH-3T3 cells, which exhibit low CD44 expression, only very weak signals were observed in Figure 6c. Moreover, as CD-44 was competing with the PFEP/FA-HA binding, we also evaluated cellular uptake efficiency with only PFEP in MCF-7 cells in order to determine whether the complex was taken up by the cell or PFEP and FA-HA enter the cells separately. As shown in Figure S5 in the Supporting Information, much weaker fluorescent signals were detected in MCF-7 cells as compared to the fluorescent signals obtained in cell imaging experiments using the PFEP/FA-HA complex. This indicated that the polymer was mainly taken up by the cell as part of the complex because the specific HA-CD44 binding helped to improve the cellular uptake efficiency. All of the above results demonstrated that the PFEP/FA-HA complex can specifically bind to CD44 proteins overexpressed on the MCF-7 cells and internalized into the cancer cells via receptor-mediated endocytosis.[9,11,13]

■ CONCLUSION

In summary, the PFEP/FA-HA complex was fabricated through electronic interactions, which gave rise to a novel method for sensitive, visual, and facile fluorescence detection of CD44 and CD44-mediated cancer cell imaging. Our method was simple and low-cost because it only required a single fluorescent label on HA through a simple and mature reaction. This method also provided greater convenience and speed of response than previously reported methods by working in a simple mechanism; that is, the efficiencies of FRET from PFEP to FA-HA were closely related with the concentration of CD44 due to specific HA-CD44 binding. Thus, if the sample and test solution containing PFEP/FA-HA were just mixed, the fluorescent signals would change from green to blue with an increase of CD44 concentration, and the results can be directly visualized using a UV illuminator. Most importantly, the use of PFEP with excellent amplification property as well as the specific interactions between HA and CD44 endowed this method with high sensitivity and specificity, making it applicable for reliable quantitative detection of CD44. Furthermore, through specific interactions between the HA located on the surfaces of PFEP/FA-HA nanoparticles and the CD44 protein overexpressed on the MCF-7 cancer cells, the complex could selectively bind to cancer cells, which was examined through a dual-color fluorescence imaging. The values of sensitivity and specificity obtained in this paper were promising and could be further improved by developing novel cationic conjugated polymers/FA-HA complex. Therefore, we believe that the development of this fluorescent probe may go

some way toward the goal of making a reliable and routine method available for early diagnosis of cancer.

■ ASSOCIATED CONTENT

Supporting Information

Un-normalized emission spectra of PFEP/FA-HA with the addition of CD44, emission spectra of PFEP/FA-HA at different molar ratio of PFEP and FA-HA, dependence of FRET ratio as a function of FA-HA concentration, dependence of ΔFRET as a function of CD44 concentration when the concentration of FA-HA was 2.5×10^{-5} M, dependence of ΔFRET as a function of CD44 concentration in the serum, and phase contrast images and fluorescent microscopic images of MCF-7 cells after incubatation with PFEP. This material is available free of charge via the Internet at http://pubs.acs.org/.

■ AUTHOR INFORMATION

Corresponding Authors

*E-mail: iamyqhuang@njupt.edu.cn. Tel.: +86 25 8586 6396. Fax: +86 25 8586 6396.

*E-mail: wei-huang@njtech.edu.cn. Fax: +86 25 5813 9988. Tel.: +86 25 5813 9001.

Notes

The authors declare no competing financial interest.

■ ACKNOWLEDGMENTS

The authors gratefully thank the financial support provided by the National Basic Research Program of China (Nos. 2009CB930601, 2012CB933301, 2012CB723402), the National Natural Science Foundation of China (Nos. 51073078, 21005040, 51173081, 51273092), the Natural Science Foundation of Jiangsu Province, China (BM2012010), the Science Foundation of Nanjing University of Posts and Telecommunications (NY213173), the Ministry of Education of China (No. IRT1148), the Priority Academic Program Development of Jiangsu Higher Education Institutions (PAPD), and the Synergetic Innovation Center for Organic Electronics and Information Displays.

■ REFERENCES

(1) Lapcik, L.; Lapcik, L.; De Smedt, S.; Demeester, J.; Chabrecek, P. Hyaluronan: Preparation, Structure, Properties, and Applications. *Chem. Rev.* **1998**, *98*, 2663−2684.

(2) Ikegami-Kawai, M.; Takahashi, T. Microanalysis of Hyaluronan Oligosaccharides by Polyacrylamide Gel Electrophoresis and Its Application to Assay of Hyaluronidase Activity. *Anal. Biochem.* **2002**, *311*, 157−165.

(3) Toole, B. P. Hyaluronan: From Extracellular Glue to Pericellular Cue. *Nat. Rev. Cancer* **2004**, *4*, 528−539.

(4) Zhang, L. S.; Mummert, M. E. Development of a Fluorescent Substrate to Measure Hyaluronidase Activity. *Anal. Biochem.* **2008**, *379*, 80−85.

(5) Choi, K. Y.; Min, K. H.; Na, J. H.; Choi, K.; Kim, K.; Park, J. H.; Kwon, I. C.; Jeong, S. Y. Self-assembled Hyaluronic Acid Nanoparticles as a Potential Drug Carrier for Cancer Therapy: Synthesis, Characterization, and in Vivo Biodistribution. *J. Mater. Chem.* **2009**, *19*, 4102−4107.

(6) Choi, K. Y.; Chung, H.; Min, K. H.; Yoon, H. Y.; Kim, K.; Park, J. H.; Kwon, I. C.; Jeong, S. Y. Self-assembled Hyaluronic Acid Nanoparticles for Active Tumor Targeting. *Biomaterials* **2010**, *31*, 106−114.

(7) Saravanakumar, G.; Choi, K. Y.; Yoon, H. Y.; Kim, K.; Park, J. H.; Kwon, I. C.; Park, K. Hydrotropic Hyaluronic Acid Conjugates: Synthesis, Characterization, and Implications as a Carrier of Paclitaxel. *Int. J. Pharm.* **2010**, *394*, 154−161.

(8) Choi, K. Y.; Min, K. H.; Yoon, H. Y.; Kim, K.; Park, J. H.; Kwon, I. C.; Choi, K.; Jeong, S. Y. PEGylation of Hyaluronic Acid Nanoparticles Improves Tumor Targetability in vivo. *Biomaterials* **2011**, *32*, 1880−1889.

(9) Cho, H. J.; Yoon, H. Y.; Koo, H.; Ko, S. H.; Shim, J. S.; Lee, J. H.; Kim, K.; Kwon, I. C.; Kim, D. D. Self-assembled Nanoparticles Based on Hyaluronic Acid-ceramide (HA-CE) and Pluronic (R) for Tumor-targeted Delivery of Docetaxel. *Biomaterials* **2011**, *32*, 7181−7190.

(10) Yoon, H. Y.; Koo, H.; Choi, K. Y.; Lee, S. J.; Kim, K.; Kwon, I. C.; Leary, J. F.; Park, K.; Yuk, S. H.; Park, J. H.; Choi, K. Tumor-targeting Hyaluronic Acid Nanoparticles for Photodynamic Imaging and Therapy. *Biomaterials* **2012**, *33*, 3980−3989.

(11) Cho, H. J.; Yoon, I. S.; Yoon, H. Y.; Koo, H.; Jin, Y. J.; Ko, S. H.; Shim, J. S.; Kim, K.; Kwon, I. C.; Kim, D. D. Polyethylene Glycol-conjugated Hyaluronic Acid-ceramide Self-assembled Nanoparticles for Targeted Delivery of Doxorubicin. *Biomaterials* **2012**, *33*, 1190−1200.

(12) Cho, H. J.; Yoon, H. Y.; Koo, H.; Ko, S. H.; Shim, J. S.; Cho, J. H.; Park, J. H.; Kim, K.; Kwon, I. C.; Kim, D. D. Hyaluronic Acid-ceramide-based Optical/MR Dual Imaging Nanoprobe for Cancer Diagnosis. *J. Controlled Release* **2012**, *162*, 111−118.

(13) Twomey, M.; Na, Y.; Roche, Z.; Mendez, E.; Panday, N.; He, J.; Moon, J. H. Fabrication of Core-Shell Nanoparticles via Controlled Aggregation of Semiflexible Conjugated Polymer and Hyaluronic Acid. *Macromolecules* **2013**, *46*, 6374−6378.

(14) Chong, H.; Zhu, C.; Song, J.; Feng, L.; Yang, Q.; Liu, L.; Lv, F.; Wang, S. Preparation and Optical Property of New Fluorescent Nanoparticles. *Macromol. Rapid Commun.* **2013**, *34*, 736−742.

(15) Ishimoto, T.; Nagano, O.; Yae, T.; Tamada, M.; Motohara, T.; Oshima, H.; Oshima, M.; Ikeda, T.; Asaba, R.; Yagi, H.; Masuko, T.; Shimizu, T.; Ishikawa, T.; Kai, K.; Takahashi, E.; Imamura, Y.; Baba, Y.; Ohmura, M.; Suematsu, M.; Baba, H.; Saya, H. CD44 Variant Regulates Redox Status in Cancer Cells by Stabilizing the xCT Subunit of System xc(−) and Thereby Promotes Tumor Growth. *Cancer Cell* **2011**, *19*, 387−400.

(16) Orian-Rousseau, V. CD44, a Therapeutic Target for Metastasising Tumours. *Eur. J. Cancer* **2010**, *46*, 1271−1277.

(17) Platt, V. M.; Szoka, F. C., Jr. Anticancer Therapeutics: Targeting Macromolecules and Nanocarriers to Hyaluronan or CD44, a Hyaluronan Receptor. *Mol. Pharmaceutics* **2008**, *5*, 474−486.

(18) Guo, Y. J.; Liu, G. L.; Wang, X. N.; Jin, D.; Wu, M. C.; Ma, J.; Sy, M. S. Potential Use of Soluble CD44 in Serum as Indicator of Tumor Burden and Metastasis in Patients with Gastric or Colon-Cancer. *Cancer Res.* **1994**, *54*, 422−426.

(19) Ristamaki, R.; Joensuu, H.; Lappalainen, K.; Teerenhovi, L.; Jalkanen, S. Elevated Serum CD44 Level is Associated with Unfavorable Outcome in Non-Hodgkin's Lymphoma. *Blood* **1997**, *90*, 4039−4045.

(20) Matsumura, Y.; Hanbury, D.; Smith, J.; Tarin, D. Noninvasive Detection of Malignancy by Identification of Unusual CD44 Gene Activity in Exfoliated Cancer-Cells. *Br. Med. J.* **1994**, *308*, 619−624.

(21) Sugiyama, M.; Woodman, A.; Sugino, T.; Crowley, S.; Ho, K.; Smith, J.; Matsumura, Y.; Tarin, D. Noninvasive Detection of Bladder-Cancer by Identification of Abnormal CD44 Proteins in Exfoliated Cancer-Cells in Urine. *J. Clin. Pathol.* **1995**, *48*, M142−M147.

(22) Martin, S.; Jansen, F.; Bokelmann, J.; Kolb, H. Soluble CD44 Splice Variants in Metastasizing Human Breast Cancer. *Int. J. Cancer* **1997**, *74*, 443−445.

(23) Lackner, C.; Moser, R.; Bauernhofer, T.; Wilders-Truschnig, M.; Samonigg, H.; Berghold, A.; Zatloukal, K. Soluble CD44 v5 and v6 in Serum of Patients with Breast Cancer. Correlation with Expression of CD44 v5 and v6 Variants in Primary Tumors and Location of Distant Metastasis. *Breast Cancer Res. Treat.* **1998**, *47*, 29−40.

(24) Darai, E.; Leblanc, M.; Walker-Combrouze, F.; Bringuier, A. F.; Madelenat, P.; Scoazec, J. Y. Expression of Cadherins and CD44 Isoforms in Ovarian Endometrial Cysts. *Hum. Reprod.* **1998**, *13*, 1346−1352.

(25) Darai, E.; Bringuier, A. F.; Walker-Combrouze, F.; Feldmann, G.; Madelenat, P.; Scoazec, J. Y. Soluble Adhesion Molecules in Serum and Cyst Fluid from Patients with Cystic Tumours of the Ovary. *Hum. Reprod.* **1998**, *13*, 2831−2835.
(26) Woodman, A. C.; Goodison, S.; Drake, M.; Noble, J.; Tarin, D. Noninvasive Diagnosis of Bladder Carcinoma by Enzyme-linked Immunosorbent Assay Detection of CD44 Isoforms in Exfoliated Urothelia. *Clin. Cancer Res.* **2000**, *6*, 2381−2392.
(27) Clevers, H. The Cancer Stem Cell: Premises, Promises and Challenges. *Nat. Med.* **2011**, *17*, 313−319.
(28) Giepmans, B. N. G.; Adams, S. R.; Ellisman, M. H.; Tsien, R. Y. Review - The Fluorescent Toolbox for Assessing Protein Location and Function. *Science* **2006**, *312*, 217−224.
(29) Cao, M. R.; Hou, J.; Zhang, Q.; Bai, F.; Bai, G. Preparation of Hyaluronic Acid-Quantum Dot Conjugate and Its Application in Tumor Imaging. *Chem. J. Chin. Univ.* **2012**, *33*, 437−441.
(30) Kim, J.; Kim, K. S.; Jiang, G.; Kang, H.; Kim, S.; Kim, B. S.; Park, M. H.; Hahn, S. K. In Vivo Real-Time Bioimaging of Hyaluronic Acid Derivatives Using Quantum Dots. *Biopolymers* **2008**, *89*, 1144−1153.
(31) Yang, J.; Zhang, Y.; Gautam, S.; Liu, L.; Dey, J.; Chen, W.; Mason, R. P.; Serrano, C. A.; Schug, K. A.; Tang, L. Development of Aliphatic Biodegradable Photoluminescent Polymers. *Proc. Natl. Acad. Sci. U. S. A.* **2009**, *106*, 10086−10091.
(32) Lee, J. S.; Green, J. J.; Love, K. T.; Sunshine, J.; Langer, R.; Anderson, D. G. Gold, Poly(beta-amino ester) Nanoparticles for Small Interfering RNA Delivery. *Nano Lett.* **2009**, *9*, 2402−2406.
(33) Lewinski, N.; Colvin, V.; Drezek, R. Cytotoxicity of Nanoparticles. *Small* **2008**, *4*, 26−49.
(34) Thomas, S. W., III; Joly, G. D.; Swager, T. M. Chemical Sensors Based on Amplifying Fluorescent Conjugated Polymers. *Chem. Rev.* **2007**, *107*, 1339−1386.
(35) Liu, B.; Bazan, G. C. Homogeneous Fluorescence-Based DNA Detection with Water-soluble Conjugated Polymers. *Chem. Mater.* **2004**, *16*, 4467−4476.
(36) Ho, H. A.; Najari, A.; Leclerc, M. Optical Detection of DNA and Proteins Moth Cationic Polythiophenes. *Acc. Chem. Res.* **2008**, *41*, 168−178.
(37) Jiang, H.; Taranekar, P.; Reynolds, J. R.; Schanze, K. S. Conjugated Polyelectrolytes: Synthesis, Photophysics, and Applications. *Angew. Chem., Int. Ed.* **2009**, *48*, 4300−4316.
(38) Huang, Y. Q.; Liu, X. F.; Fan, Q. L.; Wang, L.; Song, S.; Wang, L. H.; Fan, C.; Huang, W. Tuning Backbones and Side-chains of Cationic Conjugated Polymers for Optical Signal Amplification of Fluorescent DNA Detection. *Biosens. Bioelectron.* **2009**, *24*, 2973−2978.
(39) Huang, Y. Q.; Fan, Q. L.; Liu, X. F.; Fu, N. N.; Huang, W. Solvent- and pH-Induced Self-Assembly of Cationic Meta-Linked Poly(phenylene ethynylene): Effects of Helix Formation on Amplified Fluorescence Quenching and Forster Resonance Energy Transfer. *Langmuir* **2010**, *26*, 19120−19128.
(40) Li, J.; Huang, Y. Q.; Qin, W. S.; Liu, X. F.; Huang, W. An Optical-logic System Based on Cationic Conjugated Polymer/DNA/Intercalating Dyes Assembly for Label-free Detection of Conformational Conversion of DNA i-motif Structure. *Polym. Chem.* **2011**, *2*, 1341−1346.
(41) Liu, X. F.; Lan, O.; Cai, X. H.; Huang, Y. Q.; Feng, X. M.; Fan, Q. L.; Huang, W. An Ultrasensitive Label-free Biosensor for Assaying of Sequence-specific DNA-binding protein Based on Amplifying Fluorescent Conjugated Polymer. *Biosens. Bioelectron.* **2013**, *41*, 218−224.
(42) Liu, X. F.; Shi, L.; Hua, X. X.; Huang, Y. Q.; Su, S.; Fan, Q. L.; Wang, L. H.; Huang, W. Target-Induced Conjunction of Split Aptamer Fragments and Assembly with a Water-Soluble Conjugated Polymer for Improved Protein Detection. *ACS Appl. Mater. Interfaces* **2014**, *6*, 3406−3412.
(43) Zhu, C.; Liu, L.; Yang, Q.; Lv, F.; Wang, S. Water-Soluble Conjugated Polymers for Imaging, Diagnosis, and Therapy. *Chem. Rev.* **2012**, *112*, 4687−4735.
(44) Parthasarathy, A.; Ahn, H.-Y.; Belfield, K. D.; Schanze, K. S. Two-Photon Excited Fluorescence of a Conjugated Polyelectrolyte and Its Application in Cell Imaging. *ACS Appl. Mater. Interfaces* **2010**, *2*, 2744−2748.
(45) Chong, H.; Nie, C.; Zhu, C.; Yang, Q.; Liu, L.; Lv, F.; Wang, S. Conjugated Polymer Nanoparticles for Light-Activated Anticancer and Antibacterial Activity with Imaging Capability. *Langmuir* **2012**, *28*, 2091−2098.
(46) Jiang, R.; Lu, X.; Yang, M.; Deng, W.; Fan, Q.; Huang, W. Monodispersed Brush-Like Conjugated Polyelectrolyte Nanoparticles with Efficient and Visualized SiRNA Delivery for Gene Silencing. *Biomacromolecules* **2013**, *14*, 3643−3652.
(47) Pu, K. Y.; Liu, B. Fluorescent Conjugated Polyelectrolytes for Bioimaging. *Adv. Funct. Mater.* **2011**, *21*, 3408−3423.
(48) Feng, X.; Liu, L.; Wang, S.; Zhu, D. Water-soluble Fluorescent Conjugated Polymers and their Interactions with Biomacromolecules for Sensitive Biosensors. *Chem. Soc. Rev.* **2010**, *39*, 2411−2419.
(49) Lee, K.; Lee, J.; Jeong, E. J.; Kronk, A.; Elenitoba-Johnson, K. S. J.; Lim, M. S.; Kim, J. Conjugated Polyelectrolyte-Antibody Hybrid Materials for Highly Fluorescent Live Cell-Imaging. *Adv. Mater.* **2012**, *24*, 2479−2484.
(50) McRae, R. L.; Phillips, R. L.; Kim, I.-B.; Bunz, U. H. F.; Fahrni, C. J. Molecular Recognition Based on Low-affinity Polyvalent Interactions: Selective Binding of a Carboxylated Polymer to fibronectin fibrils of live fibroblast cells. *J. Am. Chem. Soc.* **2008**, *130*, 7851−7853.
(51) Zhu, C.; Yang, Q.; Liu, L.; Wang, S. A Potent Fluorescent Probe for the Detection of Cell Apoptosis. *Chem. Commun.* **2011**, *47*, 5524−5526.
(52) Bjork, P.; Nilsson, K. P. R.; Lenner, L.; Kagedal, B.; Persson, B.; Inganas, O.; Jonasson, J. Conjugated Polythiophene Probes Target Lysosome-related Acidic Vacuoles in Cultured Primary Cells. *Mol. Cell. Probes* **2007**, *21*, 329−337.
(53) Pu, K.-Y.; Li, K.; Liu, B. Multicolor Conjugate Polyelectrolyte/Peptide Complexes as Self-Assembled Nanoparticles for Receptor-Targeted Cellular Imaging. *Chem. Mater.* **2010**, *22*, 6736−6741.
(54) Pu, K.-Y.; Li, K.; Liu, B. A Molecular Brush Approach to Enhance Quantum Yield and Suppress Nonspecific Interactions of Conjugated Polyelectrolyte for Targeted Far-Red/Near-Infrared Fluorescence Cell Imaging. *Adv. Funct. Mater.* **2010**, *20*, 2770−2777.
(55) Huang, Y. Q.; Fan, Q. L.; Lu, X. M.; Fang, C.; Liu, S. J.; Yu-Wen, L. H.; Wang, L. H.; Huang, W. Cationic, Water-soluble, Fluorene-containing poly(arylene ethynylene)s: Effects of Water Solubility on Aggregation, Photoluminescence Efficiency, and Amplified Fluorescence Quenching in Aqueous Solutions. *J. Polym. Sci., Part A: Polym. Chem.* **2006**, *44*, 5778−5794.
(56) Belder, A. N. D; Wik, K. O. Preparation and Properties of Fluorescein-labelled Hyaluronate. *Carbohydr. Res.* **1975**, *44*, 251−257.
(57) Gaylord, B. S.; Heeger, A. J.; Bazan, G. C. DNA Hybridization Detection with Water-soluble Conjugated Polymers and Chromophore-labeled Single-stranded DNA. *J. Am. Chem. Soc.* **2003**, *125*, 896−900.
(58) Liu, B.; Gaylord, B. S.; Wang, S.; Bazan, G. C. Effect of Chromophore-charge Distance on the Energy transfer Properties of Water-soluble Conjugated Oligomers. *J. Am. Chem. Soc.* **2003**, *125*, 6705−6714.
(59) Lakowicz, J. R. *Principles of Fluorescence Spectroscopy*, 2nd ed; Kluwer Academic/Plenum Publishers: New York, 1999.
(60) Feng, X.; Lv, F.; Liu, L.; Tang, H.; Xing, C.; Yang, Q.; Wang, S. Conjugated Polymer Nanoparticles for Drug Delivery and Imaging. *ACS Appl. Mater. Interfaces* **2010**, *2*, 2429−2435.
(61) Lee, K.; Rouillard, J.-M.; Kim, B.-G.; Gulari, E.; Kim, J. Conjugated Polymers Combined with a Molecular Beacon for Label-Free and Self-Signal-Amplifying DNA Microarrays. *Adv. Funct. Mater.* **2009**, *19*, 3317−3325.
(62) Tang, Z.; Mallikaratchy, P.; Yang, R.; Kim, Y.; Zhu, Z.; Wang, H.; Tan, W. Aptamer Switch Probe Based on Intramolecular Displacement. *J. Am. Chem. Soc.* **2008**, *130*, 11268−11269.

(63) Nutiu, R.; Li, Y. F. A DNA-protein nanoengine for "On-Demand" Release and Precise Delivery of Molecules. *Angew. Chem., Int. Ed.* **2005**, *44*, 5464−5467.
(64) He, F.; Tang, Y. L.; Yu, M. H.; Feng, F.; An, L. L.; Sun, H.; Wang, S.; Li, Y. L.; Zhu, D. B.; Bazan, G. C. Quadruplex-to-duplex Transition of G-rich Oligonucleotides Probed by Cationic Water-soluble Conjugated Polyelectrolytes. *J. Am. Chem. Soc.* **2006**, *128*, 6764−6765.
(65) Liu, J.; Cao, Z.; Lu, Y. Functional Nucleic Acid Sensors. *Chem. Rev.* **2009**, *109*, 1948−1998.